



Available online at [www.sciencedirect.com](http://www.sciencedirect.com)

ScienceDirect

Procedia Earth and Planetary Science 15 (2015) 579 – 584

Procedia  
Earth and Planetary Science

World Multidisciplinary Earth Sciences Symposium, WMESS 2015

# Morphology and Radiation-induced Centres of Technogenic Gypsum

Khasanova N.M.<sup>a\*</sup>, Khasanov R.A.<sup>a,b</sup>, Nizamutdinov N.M.<sup>a</sup>, Salimov R.I.<sup>a</sup>, Izotov V.G.<sup>a</sup>

<sup>a</sup>Kazan federal university, Kazan, 420008 Russia

<sup>b</sup>Central Research Institute for Geology of Industrial Minerals, Kazan, 420097 Russia

## Abstract

Gypsum crystals were formed from a saturated solution of produced water remaining in the horizontal section of the discharge pipe and cause undesired (side) man-made phenomenon as clogged pipe. However, for scientific purposes, this fact has become unique and revealed the typical defect centres, and enable us to study the effect of thermal and radiation effects on the crystal structure gypsum. Single crystals of gypsum at room temperature may gradually lose crystallization water. Its absence is compensated by the change of coordination number, calcium, and sulfur, which leads to the formation of point defects, which become paramagnetic during irradiation. It was found that the morphology of single crystals of gypsum corresponds to setting I2/a monoclinic system. The faces of the crystal are allocated on a well-developed cleavage plane (010) perpendicular to the axis b. Face, elongated along the [100] direction, was used to identify the orientation of the crystal in the resonator of electron paramagnetic resonance (EPR) spectrometer. In this paper, parameters of the spin Hamiltonian of paramagnetic centres and their models in a crystal of technogenic gypsum were presented. They are suitable for reliable ESR dating and reconstruction of the environment.

© 2015 The Authors. Published by Elsevier B.V. This is an open access article under the CC BY-NC-ND license

(<http://creativecommons.org/licenses/by-nc-nd/4.0/>).

Peer-review under responsibility of the Organizing Committee of WMESS 2015.

**Keywords:** Gypsum; annealing; electron paramagnetic resonance; X-rays; ion-radicals.

## 1. Introduction

In nature, gypsum is produced in various ways. Considerable quantities are usually deposited by sedimentary, in the initial stages of salt evaporation basins drying, or arise as a result of hydration of anhydrite in sediments under the influence of surface water under reduced external pressure (Betekhtin, 1950). At the same time, together with other

\* Corresponding author. Tel.: +7 843 292-70-62.

E-mail address: [nailiakhasanova@gmail.com](mailto:nailiakhasanova@gmail.com); [nkhasano@yandex.ru](mailto:nkhasano@yandex.ru)

sulphates gypsum is often found in oil fields and with native sulfur attributed to sedimentary deposits. Gypsum is an autogenic mineral. It is widely used as a "marker" in palaeohydrology, climatology and geochronology. Possibilities of using it as a marker have significantly increased with the use of electron paramagnetic resonance (EPR) and infrared (IR) spectroscopy (Nagar et.al, 2010), and thermoluminescence (TL) (Aydas et.al., 2011). For example, a study of the chronology of the fibrous gypsum deposited in cracks and fractures in areas subjected to strong tectonic effects by EPR spectra, has become important in determining the risk of earthquakes (Mathew et.al., 2004). Most new trend relate to the use of crystallization water as a source for plants (Palacio et.al., 2014). Many physical properties of gypsum are connected or controlled by water molecules (Knight, et.al.1999). Single crystals of gypsum may gradually lose crystallization water at room temperature. The deficiency of this water is accompanied by a change in the coordination number of calcium, sulfur, and the formation of vacancies Ca, O, and water molecules. As a result, the formation of point defects in the crystal structure, which turn paramagnetic under natural or artificial irradiation are the subject of study by EPR (Gunter, 1967; Antonio et.al., 1982; Kasuya et al., 1991; Jkeda and Jkeya, 1992; Khasanov et al., 2008; 2014). For the purposes of establishing reference markers of gypsum crystals for different generations in solving scientific and applied problems, it is relevant to search and identify them in a stable paramagnetic centre (PC). In this paper, technogenic gypsum crystals were investigated regarding the influence X-ray irradiation and thermal annealing on EPR properties.

## 2. Technogenic gypsum and its morphology

Gypsum crystals were formed from a saturated solution of produced water remaining in the horizontal section of the discharge pipe as a result of stopping the pump in the hot summer of 2010. They have become an undesirable technogenic phenomenon, as the clogged pipe had to be replaced. The saturation anions and cations were ( $\text{HCO}_3^-$  - 0.05%;  $\text{SO}_4^{2-}$  0.19%;  $\text{Cl}^-$  -49.76%) and ( $\text{Ca}^{2+}$  -6.15%;  $\text{Mg}^{2+}$  -4/33%; Na + K -39/52%) according to chemical analysis, respectively. The total iron content was 0.24 mg per one  $\text{dm}^3$  and the solution was of pH = 4.95.

The morphology of the crystals depends on internal and external factors. The first is determined by the crystal structure and space group symmetry. The second are the conditions of saturation and temperature of the solution, the presence of impurities and catalysts or inhibitors that are directly determined by crystal habit and the selection of crystal setting. In practice, I2/a-setting is different from C2/c-setting meaning monoclinic angle  $\beta = 118.43^\circ$  and the  $\beta = 114.17^\circ$ , respectively. The morphology of technogenic gypsum crystals has been studied and found it appropriates settings I2/a monoclinic system. Faceting of the crystal stands out a well-developed cleavage plane (010) perpendicular to the b axis of the crystal (Fig. 1a).

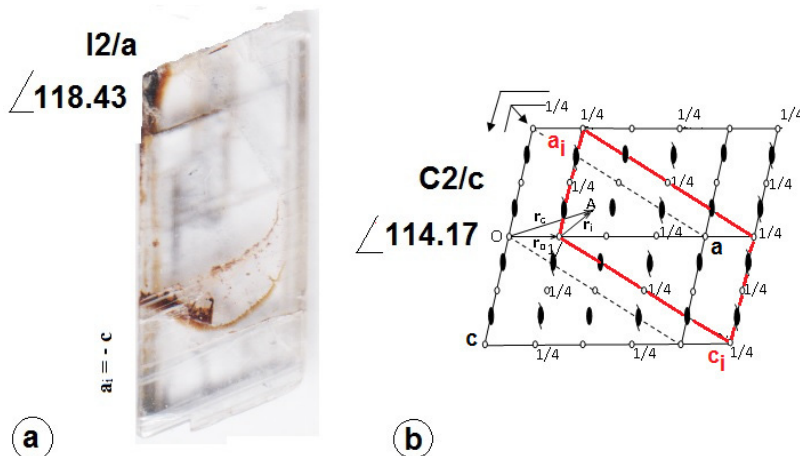


Fig. 1. Gypsum technogenic - a); Unit cell axes to set C2/c (abc) and I2/a (a<sub>1</sub>b<sub>1</sub>c<sub>1</sub>) space group C<sub>2h</sub><sup>6</sup> at (010) - b).

This facet is elongated along the [100] direction, that allows to use it to identify the orientation of the crystal in the cavity of the EPR spectrometer. However, the analysis program structures are given in the standard setting, so consider the features of the transition from one setting to another.

The structure of the space group  $C_{2h}^6$  are described in the standard setting  $C2/c$  by using basis vectors **a**, **b**, **c** at the origin coinciding with the centre of inversion in the plane type **c** (Fig.1b) (International Tables for Crystallography, 1988). The basis vectors (**a**, **b**, **c**) in **C**- setting and (**a<sub>i</sub>**, **b<sub>i</sub>**, **c<sub>i</sub>**) in **I**-setting are connected with relations: **a<sub>i</sub>** = - **c**, **b<sub>i</sub>** = **b**, **c<sub>i</sub>** = **a** + **c**; or **a** = **a<sub>i</sub>** + **c<sub>i</sub>**, **b** = **b<sub>i</sub>**, **c** = - **a<sub>i</sub>**. Space group allows four types of regular points 4a, 4b, 4c, 4d to the position of group  $G_a = C_i$ . Type point 4a and 4b belong to the plane type **c**, but point-type 4c and 4d belong to the plane type **n**. In crystallography, it is decided to use the right coordinate system and the angle  $\beta$  is selected more than  $90^\circ$ . On (Fig. 1b) shows that **I**- cell can be selected with the origin at the centre of inversion in the plane type **c** as well as **n**. The axis of the second order will be determined by the coordinates of the positions  $\frac{1}{4}y$  0 if the origin is at the centre of the inversion plane **c**-type and coordinates  $\frac{1}{2}y$   $\frac{1}{4}$  if the origin is at the centre of the **n**-type. If the coordinates of Ca atom in **I**-setting are  $\frac{1}{2}$  0.07968  $\frac{1}{4}$  (Pedersen, Semmingsen, 1982), then the origin is chosen in the plane of the **n**-type, in the centre of inversion at the height of  $\frac{1}{4}$  of the plane of the drawing. The origin coordinate will be shifted relative to each other in settings  $C2/c$  and  $I2/a$  by the vector  $\mathbf{r}_0 = x_0\mathbf{a} + y_0\mathbf{b} + z_0\mathbf{c}$ , where -  $x_0 = \frac{1}{4}$ ,  $y_0 = \frac{1}{4}$ ,  $z_0 = 0$ . Computed coordinates of the atoms of gypsum to set  $C2/c$  are used (Khasanov, 2008).

### 3. Radiation-induced centres of technogenic gypsum

The X-ray irradiation of crystals (3 h and 18 mA, 30 kV, URS: 55A,  $\lambda\text{CuK}\alpha$ ) has stimulated the EPR PC (Fig. 2), which were observed earlier in natural gypsum and described as centres A, B, C (Antonio, 1982) and G1, G2, G3, G4 (Kasuya et al., 1991; Jkeda and Jkeya, 1992). The angular dependence of the EPR spectra in three orthogonal planes (**c**; **a\***; **b**) in the technogenic gypsum (Fig. 3) was carried out with a step 5-10 degrees.

The calculation of the EPR spectra included determination of the parameters of the spin Hamiltonian (SH), positions and intensities of the lines was performed using a numerical matrix diagonalization SH (Mombourquette et.al., 1996). The value and the direction of the principal axes of the g-tensor computing for PC G1, G2, G3 technogenic gypsum are shown in (Table). Hereinafter, the features of each PC in the technogenic gypsum are isolated and are compared with known models.

G1-  $\text{SO}_3^-$ . PC presented a broad line G1 in the EPR spectrum technogenic gypsum (Fig. 2, 3) and the g-tensor parameters (Table) was identified as ion-radical  $\text{SO}_3^-$  and described more detail (Khasanov, 2008). It is important to note that this radical is characterized by the number of magnetic conjugate ( $K_M$ ) spectra equal to two and formed due to vacancies of O(1) oxygen tetrahedron structural  $\text{SO}_4^{2-}$  and  $\text{Ca}^{2+}$  nearest to a given oxygen. The local symmetry centre is reduced to  $C_1$ .

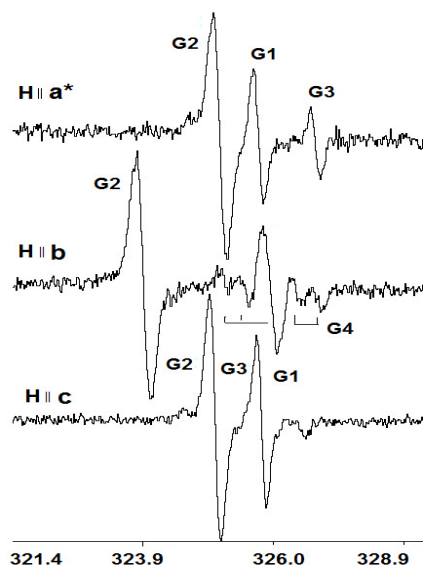


Fig. 2. The EPR G1, G2, G3, G4 with magnetic field H along orthogonal axes **a\*****b****c** of the technogenic gypsum.

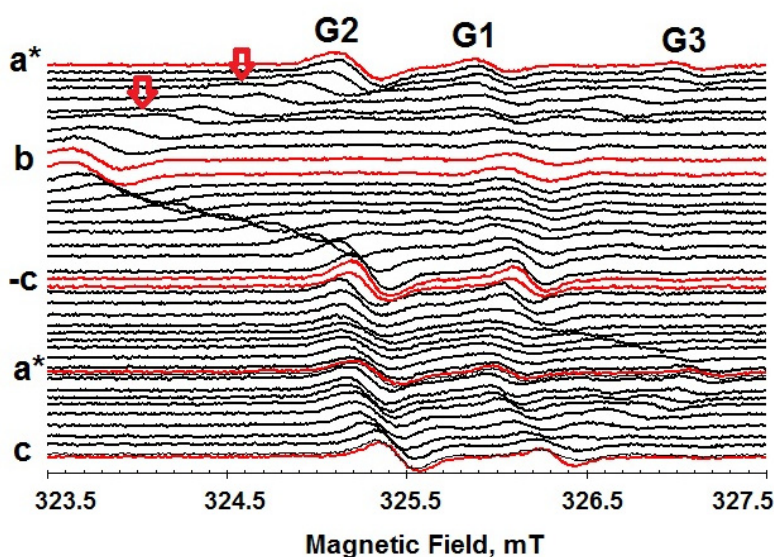


Fig. 3. The EPR angular dependence of G1, G2 and G3 in three orthogonal planes of the technogenic gypsum. The arrow indicate point splitting the super hyperfine splitting of protons ( $I=1/2$ ).

G4 -  $\text{SO}_3^-(\text{A1})$  и  $\text{SO}_3^-(\text{A2})$ . Two doublet lines G4 are clearly visible when the magnetic field is oriented along the b-axis (Fig. 2). The intensities of lines G4 centres are small compared to the G1 centre and similar lines in gypsum "Marino Steklo" (Khasanov, 2008). To identify the lines of the doublet the gypsum crystals "Marino Steklo" were irradiated with X-rays and the angular dependence of the EPR spectra was studied in three orthogonal planes (Khasanov, 2014).

Moreover, during thermal annealing (30 min) and subsequent recording of spectra along the b-axis of the crystal after every 10 °C found a significant decrease in the intensity of extreme lines A1 versus A2 with internal. The small deviations of the principal values of the g-tensor centres of A1 and A2 from 2.0023 were allowed to attribute these centres ion radicals  $\text{SO}_3^-(\text{A1})$  and  $\text{SO}_3^-(\text{A2})$ . The direction of the principal axis of the g-tensor close to direction of S-O(1) for both the radical ions  $\text{SO}_3^-(\text{A1})$  and  $\text{SO}_3^-(\text{A2})$  has been established. In contrast to the direction of the maximum principal axis of the tensor super fine interaction was proved different for each PC. For ion-radical  $\text{SO}_3^-(\text{A1})$  this direction was close to the direction S - H(2) proton of the water molecule adjacent layer at a distance of ~ 3,13Å. But in the case of ion-radical  $\text{SO}_3^-(\text{A2})$  maximum splitting is assigned to proton H(1) water molecules adjacent chain corrugated layer at a distance of S-H(1) ~ 3.96 Å.

Table 1. Principal values and directions of the axes g-tensor PC in technogenic gypsum

PC	axis	Principal axis g-tensor			
		value $g_{ii}$	direction, degree		
G3- $\text{SO}_3^-$	$g_{xx}$	2.0029(4)	79.6	72.2	20.8
	$g_{yy}$	2.0025(7)	24.1	114	92.5
	$g_{zz}$	2.0035(7)	68.5	30.6	110.7
	$g_{iso}$	2.0030(2)			
G2- $\text{SO}_4^-$	$g_{xx}$	2.0076(7)	10.4	80.0	93.0
	$g_{yy}$	2.0069(7)	99.7	10.6	85.7
	$g_{zz}$	2.0175(2)	86.3	93.7	5.3
	$g_{iso}$	2.0107(2)			
G3- $\text{CO}_2^-$	$g_{xx}$	2.0022(7)	11.2	85.5	79.7
	$g_{yy}$	1.9956(1)	94.1	4.9	92.6
	$g_{zz}$	2.0014(0)	100.4	88.2	10.6
	$g_{iso}$	1.9997(6)			

G2 -  $\text{SO}_4^-$ . The most intense lines G2 with a half-width of 0.2-0.3 mT and large g-tensor anisotropy is observed in the EPR of technogenic gypsum (Fig. 2 and 3). The principal values and direction of the axes g- tensor are shown in (Table). They belong to the axial symmetry PC with the number  $K_M = 2$ . For the spectral lines in the plane  $ba^*$  is observed splitting in the range of 40 degree angular dependence due to the interaction the unpaired electron with the proton (nuclear spin  $I = 1/2$ ) of the hydrogen atoms (marked by the arrows in Fig. 3). This splitting was related to the multiplicity magnetic centres appearance in (Kasuya et al., 1991). It should be noted that the orientation of the principal axes of the ion-radical are close are close to each other PC G2  $\text{SO}_4^-$  (Jkeda and Jkeya, 1992, Nagar et.al., 2010), but differs in the value of the principal component of the g - tensor. In cited papers the principal values are determined from EPR spectra in the gypsum powder:  $g_{xx} = 2.0084$ ;  $g_{yy} = 2.0088$ ;  $g_{zz} = 2.0192$  (Jkeda and Jkeya, 1992), and  $g_{||} = 2.0192$ ;  $g_{\perp} = 2.0088$  (Nagar et.al., 2010). We can assume that the absence of exact coincidence of values associated with the ability to calculate the component g - tensor in crystal and powder, and also a variety of charge compensation of natural crystals.

$G_{zz} = 2.0175$  axis deviates from the axis of symmetry of the crystal  $L_2$  by about 5 degrees pointing to the  $\text{Ca}^{2+}$  cation in the immediate environment The other two principal directions of the axes are located near the plane of symmetry of the crystal. The ion-radical  $\text{SO}_4^-$  at plane  $ba^*$  has in its environment protons, splitting the spectral lines of the EPR. At planes  $ca^*$  and  $bc$  the influence the proton environment is weaker and only leads to a broadening of the spectral lines. Charge compensation of ion-radical  $\text{SO}_4^-$  was carried out due to volumetric charge redistribution.

G3- $\text{CO}_2^-$ . Electronic PC in the accordance with the parameters g- tensor in (Table) and the direction of the principal axes close to the direction of the crystallographic axes of gypsum similar to G3 (Fig. 2 and 3). The EPR spectrum of the centre is composed of one broadened line of low intensity. The observed broadening is probably due to the interaction of the unpaired spin electron with the nuclear spins of the proton environment. The best agreement

between the experimental and theoretical values of the spectral lines is achieved by assuming the multiplicity of  $K_M = 2$  because of the lowering of the symmetry centre to  $C_1$ . This centre is identified as  $CO_2^-$  (Kasuya et al., 1991; Jkeda and Jkeya, 1992). Directions g-tensor principal axes indicate that the centre is deployed relative to the position of the original tetrahedron of gypsum (Table). One can assume that in the model observed  $CO_2^-$  are involved oxygen O(1) of the tetrahedron.

#### 4. Thermo-radiation effect on technogenic gypsum

The annealed crystal was held in a dry atmosphere of carbon monoxide for 30 minutes at 90 and 110 °C. The irradiation with X-rays and recording the EPR occurred in air at room temperature. A total of eight thermo-radiation treatments were performed in the following order: annealing at 90 °C, X-ray irradiation, annealing at 90 °C, X-ray irradiation, pause for 48h, pause 24h, annealing at 110 °C and X-ray irradiation. After each procedure, the EPR spectra of the magnetic field along orthogonal axes (bca\*) of the crystal was scanned. Changes in intensity relative to the original sample of each line were calculated and are presented in chart form on (Fig. 4).

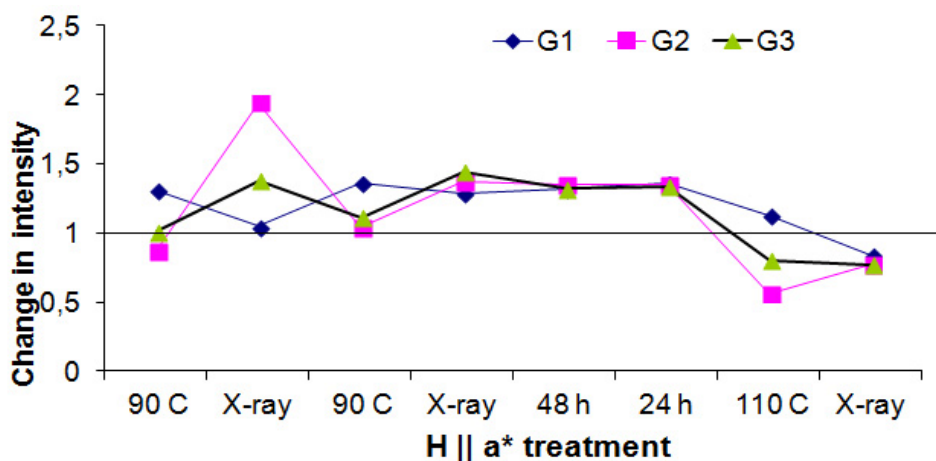


Fig. 4. Diagram of the relative change in the intensity PC G1, G2, G3 during the thermal annealing and X-ray irradiation treatments as follows: 90 °C, X-ray, 90 °C, X-ray, pause of 48 h and 24 h, 110 °C and X-ray.

The studies of the thermal expansion tensor in gypsum have shown that the maximum anisotropy tensor is observed in the direction of the crystal axis b. Changes in the gypsum crystal cell with temperature was explained the weakening of the hydrogen bond H2 - O1, which is oriented almost parallel to the axis b (Knight, et.al.1999).

#### 5. Conclusion

Heating the crystal to 90°C contributed to the disappearance of doublet lines G4-  $SO_3^-$  (A1) and  $SO_3^-$  (A2). They are not recovered after X-ray irradiation. The presence of the EPR PC  $SO_3^-$  allows the appearance of the gypsum structure spheres with a radius of  $\sim 4\text{\AA}$ , inside which there are no water molecules. This model PC G1 is in agreement with of change intensity (Fig.4): - increase in intensity during heating and reduction upon irradiation. When heated to 90°C there is increasing mobility of molecular water and the number of centres in  $SO_3^-$ . With X-ray irradiation, there is an excess of electrons, which leads to a reduction in G1, while other PC - hole G2 and electron in G3 increases. Heating to 110°C results in a decrease of intensity of the entire PC, which indicates the occurrence of a profound change in the structure of the activation of dehydration (Khasanov et al., 2008; 2014).

Thus, the crystallization conditions of arid technogenic gypsum is characterized by its own set of electron-hole centres. Man-made gypsum is an analog of the natural mineral known, and his PC markers correspond to an arid environment (Kasuya et al., 1991). SH parameters were found and the established model centres in the single crystal technogenic gypsum suitable for reliable of the EPR dating and reconstruction of the environment.

## Acknowledgment

This work was funded by the subsidy of the Russian Government to support the Program of competitive growth of Kazan Federal University among world-class academic centres and universities.

## References

1. Albuquerque, A.R.P.L., Isotani, S., 1982. The EPR spectra of X-ray irradiated gypsum, *J. Phys. Soc. Japan*, 51(4): 1111-1118.
2. Aydas, C., Engin, B., Aydin, T., 2011. Radiation-induced signals of gypsum crystals analyzed by ESR and TL. *Nuclear Instruments and Methods in Physics Research B*, 269: 417-424.
3. Betekhtin, A.G., 1950. *Mineralogy*. Moscow Gos. Izd Geol. Lit., 956 p. (In Russian)
4. Gunter, T.E., 1967. Electron Paramagnetic Resonance Studies of the Radiolysis of  $H_2O$  in the Solid State. *J.Chem.Phys*, 46 (10): 3818-3828.
5. International Tables for Crystallography. Brief Teaching Edition of Volume A. Edited by Theo Hahn. 1988.
6. Jkeda, S. and Jkeya, M., 1992. Electron spin resonance (ESR) signals in natural and synthetic gypsum: an application of ESR to the age estimation gypsum precipitates from San Andreas Fault. *Japanese Journal of Applied Physics*, 31: L136-138.
7. Kasuya M., Brumby S. and Chappell J., 1991. ESR signals from natural gypsum single crystals: Implications for ESR dating. *Nucl. Tracks Radiat. Meas.*, 18(3): 329–333
8. Khasanov, R.A., Nizamutdinov, N.M., Khasanova, N.M., Gubaidullin, A.T., Vinokurov, V.M., 2008. Low-Temperature Dehydration of Gypsum Single Crystals. *Crystall. Rep.*, 53(5): 806-811.
9. Khasanov, R.A., Nizamutdinov, N. M., Khasanova, N. M., Salimov, R.I., Kadyrov, R.I., Vinokurov, V.M., 2014. Phase States of the Gypsum Thermal-Annealing Derivatives According to Electron Spin Resonance Spectra. *Crystall. Rep.*, 59(3): 399–406.
10. Knight, K.S., Stretton, I.C., Schofield, P.F., 1999. Temperature evolution between 50 K and 320 K of the thermal expansion tensor of gypsum derived from neutron powder diffraction data. *Phys Chem Minerals*, 26: 477–483.
11. Mathew, G.T.K. Gundu Rao, P.S.Sohoni and R.V.Karanth, 2004. ESR dating of interfault gypsum from Katrol hill range, Kachchh, Gujarat: Implications for neotectonism. *Current Science*, 87(9):1269-1274.
12. Mombourquette, M.J., Weil, J.A., McGavin, D.G., 1996. *EPR-NMR USER'S Manual*. Department of Chemistry, University Saskatchewan. Canada.
13. Nagar, Y.C., Sastry, M.D., Bhushan, B., Kumar, A., Mishra, K.P., Shastri, A., Deo, M.N., Kocurek, G., Magee, J.W., Wadhawan, S.K., Juyal, N., Pandian, M.S., Shukla, A.D., Singhvi, A.K., 2010. Chronometry and formation pathways of gypsum using Electron Spin Resonance and Fourier Transform Infrared Spectroscopy. *Quaternary Geochronology*, 5(6): 691-704.
14. Palacio, S., Azorín, J., Martí, G.M., Ferrio, J.P., 2014. The crystallization water of gypsum rocks is a relevant water source for plants. *Nature Communications* [5:4660] DOI:10.1038 /ncomms5660| www.nature.com/naturecommunications
15. Pedersen, B.F., Semmingsen, 1982. Dag Neutron Diffraction Refinement of Structure of Gypsum,  $CaSO_4 \cdot 2H_2O$ . *Acta Cryst.*, B 38: 1074-1077.